DTIC FILE COPY (4)

ARL-MAT-R-120 AR-004-585

AD-A196 264

DEPARTMENT OF DEFENCE

DEFENCE SCIENCE AND TECHNOLOGY ORGANISATION

AERONAUTICAL RESEARCH LABORATORY

MELBOURNE, VICTORIA

Aircraft Materials Report 120

THE DEVELOPMENT OF ACOUSTIC EMISSION FOR STRUCTURAL INTEGRITY MONITORING OF AIRCRAFT (U)

by

C.M. SCALA, S.J. BOWLES and I.G. SCOTT

Approved for Public Release

JANUARY 1988

AR-004-585

DEPARTMENT OF DEFENCE
DEFENCE SCIENCE AND TECHNOLOGY ORGANISATION
AERONAUTICAL RESEARCH LABORATORY

Aircraft Materials Report 120

THE DEVELOPMENT OF ACOUSTIC EMISSION FOR STRUCTURAL INTEGRITY MONITORING OF AIRCRAFT

by

C.M. SCALA, S.J. BOWLES and I.G. SCOTT*

SUMMARY

This paper reviews procedures for distinguishing between acoustic emission (AE) from fatigue crack propagation and from spurious sources in aircraft applications. Particular emphasis is placed on the development at Aeronautical Research Laboratory (ARL) of procedures applicable during AE monitoring of complex-shaped components. Firstly, procedures to eliminate extraneous sources are evaluated, including the use of guard sensors and source location systems. The capabilities of additional signal-processing (which in principle can range from adaptive to non-adaptive) for identifying and locating AE from fatigue crack propagation are then evaluated. The problems in applying adaptive processing are illustrated by AE results from a Macchi aircraft in-flight and a Mirage aircraft during full-scale fatigue testing. The ARL development of semi-adaptive processing based on background research on AE sources, sensors, calibration and other techniques is also described. The successful application of this processing to the Mirage test above is then detailed, and the value of using reduced adaptation in processing is demonstrated. Finally, factors affecting future in-flight AE monitoring are discussed.

* retired

DSTO ARL
MELBOURNE

POSTAL ADDRESS: Director, Aeronautical Research Laboratory,
P.O. Box 4331, Melbourne, Victoria, 3001, Australia

CONTENTS

INTRODUCTION

The high performance of modern military aircraft is achieved largely by using materials which are at the forefront of development in materials technology. Advanced concepts, such as damage tolerance, are applied to assure airworthiness of structural components made from such materials. However, a requirement for the application of airworthiness procedures based on damage tolerance in aircraft components is the availability of reliable nondestructive inspection (NDI) techniques for the detection, monitoring and sizing of sub-critical defects.

In principle, NDI–monitoring of crack growth should be achievable using a range of techniques including strain measurements, ultrasonic testing, eddy-current inspection and acoustic emission (AE). The AE technique holds particular promise[1], viz. (i) defects can be monitored in complex-shaped components; (ii) the defects can be in inaccessible locations, e.g. beneath cover plates or on the curved surfaces of holes; (iii) precise knowledge of the exact location of the defects is not needed; (iv) defects significance can be assessed continuously. However, particular problems can be expected when applying AE to aircraft monitoring[2], e.g. (i) special techniques are needed to separate damage-related AE signals and AE from the many highly active spurious sources; (ii) a defect-related AE source in a complex-shaped aircraft component cannot be identified directly on the basis of features obtained from the source in a laboratory specimen; (iii) the free space in modern aircraft is often extremely limited, necessitating the development of special AE equipment for flight applications.

The main purpose of this paper is to review the procedures for distinguishing between AE sources in aircraft applications. Particular emphasis is placed on the development at Aeronautical Research Laboratories (ARL) of procedures applicable for AE monitoring of complex-shaped aircraft components not readily inspected in situ by more conventional NDI techniques. The ARL research has included AE monitoring of a Macchi trainer aircraft in-flight[3] and a Mirage jet-fighter aircraft during full-scale fatigue testing [4 5] as well as both theoretical [6] and experimental [7 8] background studies. Related developments at other laboratories, including AERE Harwell [9 10], Royal Military College Kingston [11 12], Lockheed, Battelle Pacific Northwest Laboratories and Rockwell Science Centre [13 14] are also discussed in context.

DISTINGUISHING BETWEEN AE SOURCES

Many spurious AE sources are likely to be active in an aircraft during flight [15] or fatigue-testing [16], e.g. sources associated with gas flow, electomagnetic interference, hydraulic noise, mechanical noise, transient electronic noise, local debonding of composite repair patches and fretting (of crack faces, of bolts in holes, of other attachment fixtures and between components such as a wing-skin and a wing-spar). Hence, considerable signal-processing is required to distinguish between such sources and AE from fatigue crack propagation.

DEVELOPMENT OF AE MONITORING OF AIRCRAFT

[2]

Elimination of Extraneous Sources

Of the many spurious sources above, vibration signals usually occur below 100 kHz, whereas AE from fatigue crack propagation contains frequency components up to many megahertz. Hence, filtering can be used to distinguish between these sources. Moreover, modern AE equipment is usually adequately protected against transient electromagnetic interference signals which usually occur at very high frequencies.

Source location systems can locate AE sources (whether spurious or damage-related) within, and reject extraneous sources from outside, a region of interest. Differences in arrival times of elastic waves at an array of sensors are measured, a wave speed is assumed and algorithms are used to calculate the location of the AE source. Some location systems assign co-ordinates to the source while others assign it to a zone within the region of interest.

Source location is most readily achieved in simple structures where the mode of wave propagation is known [17,18]. However, problems arise in complex-shaped aircraft components where wave propagation occurs as multiple combinations of longitudinal, shear and Rayleigh waves. The type of wave detected by each sensor in an array depends on the magnitude of the AE source, the sensor sensitivity to different wave modes, the relative locations of source and sensor, and the effects of boundaries on the presence of reflected or mode-converted waves. Hence, AE source location in an irregular 3-D structure generally requires an extensive sensor array, complicated algorithms and time-consuming computation.

Guard sensors can be used in combination with a sensor array to limit the detection of AE sources extraneous to a region of interest. Noise sources external to the array are identified and a guard sensor is mounted between the unwanted source and the sensor array; AE events reaching the guard sensor before reaching the array are rejected. Alternatively, rejection is controlled by measuring differences in time of flight between guard and array sensors. The effectiveness of guard sensors depends on factors such as accuracy of the wave speed used for calculation of time of flight, the number of guard sensors used and the activity of any extraneous sources.

Our experience has shown that (i) highly active extraneous sources (which are often difficult to locate and identify) are prevalent in aircraft applications, (ii) the use of large number of guard sensors is often insufficient to eliminate the detection of AE from all extraneous sources, (iii) assignment of a suitable wave speed for accurate source location in a complex structure is difficult, and (iv) spurious sources (e.g. fretting) within the region of interest cannot be eliminated by source location in a complex-shaped structure. Clearly, additional signal processing is needed to distinguish between AE signals from crack growth and other possible sources in aircraft applications.

Identification of Fatigue Crack Propagation

In principle, signal processing additional to that described above can range from adaptive processing, involving empirical analysis of large quantities of AE data on the basis of no knowledge of AE source characteristics, to non-adaptive processing, involving quantitative analysis of well-defined AE data using extensive a priori information [14] on AE source characteristics. In practice, the selection of suitable processing depends upon the availability and usability of such a priori information [5].

Non-adaptive processing appears relatively straight-forward when an "ideal" sensor (having a calibrated, wide-band response to a simple, physical parameter such as displacement normal to a surface) is used for the AE measurements and a simple-shaped structure is under investigation [1]. However, non-adaptive processing is usually not feasible in aircraft applications due to the limited information available both on AE sources in aircraft materials and on the wide range of possible spurious sources. Moreover, much of the known information (e.g. the directivity pattern of a microcrack source) is not measurable in complex-shaped components.

Adaptive signal processing is based on applying empirical pattern recognition analysis to extract the features of possible AE sources from training sets of data [14 19 20]. Source discrimination in an arbitrary data set is then undertaken using an appropriate combination of features to achieve an "acceptable" error rate. Application of this statistical approach has not been particularly successful because (i) well-defined data sets from likely sources (e.g. crack face rubbing) are not usually available for analysis, and (ii) propagation-and sensor-related (rather than source-related) features tend to be extracted from the training sets. Nevertheless, given the lack of alternatives, early ARL studies on complex-shaped structures (see below) were based on applying simple adaptive processing to an AE training set from an aircraft component to obtain an empirical relationship between crack growth and an AE parameter. This relationship could then be used to monitor the same type of component in a fleet of aircraft, if required.

ADAPTIVE AE MONITORING

The In-flight Monitoring of a Macchi Aircraft

Royal Australian Air Force (RAAF) Macchi jet-trainer aircraft are being flown under a safety-by-inspection procedure whereby growing fatigue cracks in bolt holes in the centre-section assembly tension spar are monitored using a magnetic rubber inspection technique. AE equipment developed by Battelle Pacific Laboratories was installed to monitor this region in flight [3]. The compact AE system comprised 2 sensors for source location into zones by time-of-flight measurements. Sensors resonant at 400 kHz were selected to minimize the effects of aircraft noise. One sensor was used to detect AE events, with the in-flight AE data being stored in an EPROM for later analysis at ARL. For most of the in-flight AE monitoring, a zone surrounding bolt hole 20 (at which maximum crack growth had previously occurred) was monitored (Fig.1). The zone surrounding bolt hole 19 (which was expected to be crack-free) was also monitored for several short periods, with the aim of obtaining a training set for AE from bolt-fretting in the absence of cracking.

Finally, the spar was removed from the aircraft for routine maintenance and was monitored by AE during laboratory fatigue testing to failure, without brackets, panels and bolts in place [21]; this testing provided for analysis a training set comprising AE from crack growth and (possibly) crack face rubbing and sources associated with the loading rig.

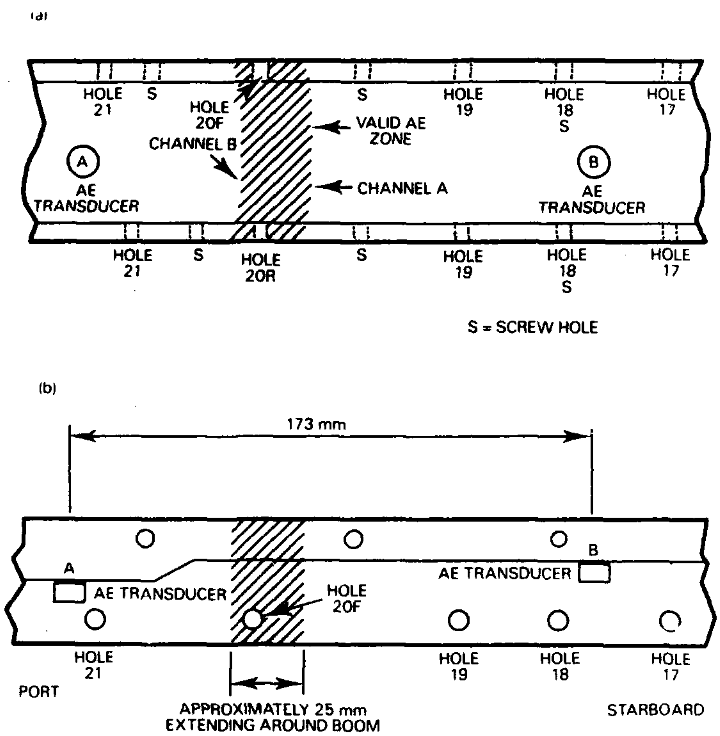

FIGURE 1 Location of AE sensors and zone (hatched area) encompassing hole 20 for Macchi wing centre section assembly boom: (a) plan view and (b) side elevation[21].

During flight, hole 19 gave considerable AE, but was also found to contain cracks. Hence, use of this training set for AE from bolt-fretting was invalid. Furthermore, a complicated relationship was obtained between AE events and the crack growth rate in hole 20, with considerably different behaviour being observed under flight and laboratory conditions (Fig.2). While these differences could have been defect-related, the results are open to a number of interpretations [21], given the different loading conditions used in two cases, the absence of bolts during fatigue testing, etc. Clearly, a more advanced approach to the acquisition and analysis of AE data was required to distinguish between sources in aircraft applications, rather than relying on the two sensor source location system and simple processing of AE events.

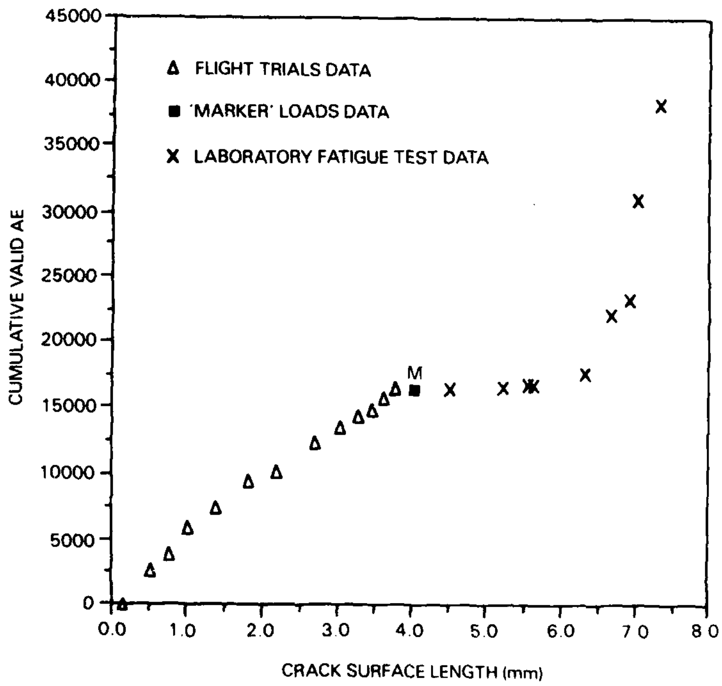

FIGURE 2 Cumulative valid AE events versus total crack surface length in hole 20 for duration of flight trials and laboratory fatigue testing. The first point (M) of laboratory data corresponds to application of "marker" load sequence[21].

The Full-scale Testing of a Mirage Aircraft

Adaptive processing was also applied in the AE monitoring of slow fatigue crack propagation in fatigue-critical holes in wing RH79 in a Mirage aircraft undergoing full-scale fatigue testing. However, the AE system developed for this test by Battelle (under ARL contract) incorporated guard sensors and a more extensive source location system than had been used in the Macchi study, and also allowed the acquisition of parametric AE data [22].

The Mirage fatigue test was carried out at the Swiss Federal Aircraft Factory (F+W), Emmen, where the aircraft was subjected to loading variable in both amplitude and frequency to simulate flight conditions. The 26 holes monitored by AE were in the bottom flange of the main wing-spar of wing RH79 (Fig.3) (this region is subsequently referred to as the critical part of the flange). Close-tolerance fasteners were used in the rear flange holes, with holes 1 to 5 also containing interference-fit stainless steel bush inserts; interference-fit fasteners were used in the forward flange holes.

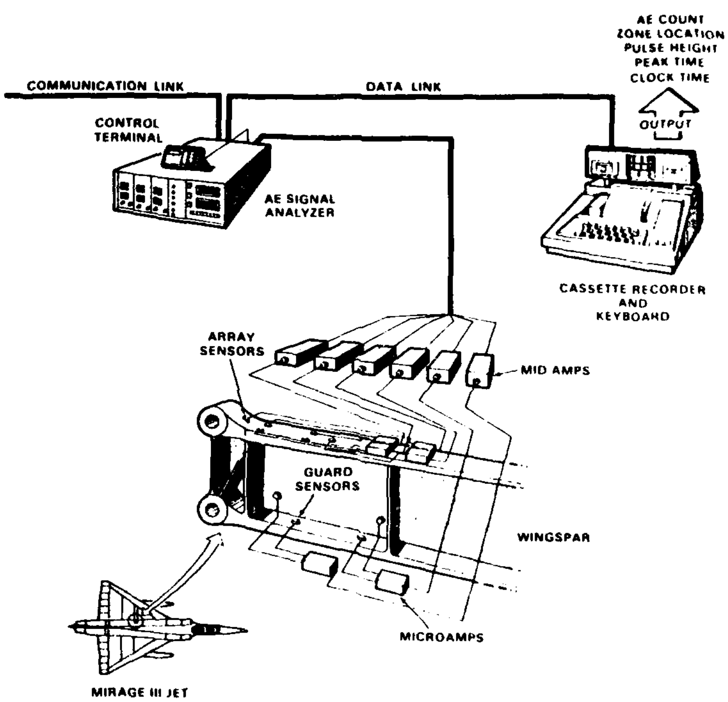

FIGURE 3 The AE zone location and guard systems used to monitor Mirage wing RH79.

Nine guard sensors were used to minimize the detection of sources extraneous to the critical part of the bottom flange and a 6-sensor array was used to locate sources within 20 zones in the critical part of the flange (Figs. 3&4). The parametric data collected were the pulse height (PH) and peak time (PT) of AE events detected at a resonant sensor located at A (Fig.4), the zone number assigned to the event and the time in seconds relative to the start of the test.

The PH and PT data obtained from the Mirage wing RH79 were complex, with several sources appearing to contribute to the AE detected in each zone. However, rather than being related to source characteristics, the AE data were clearly dominated by the effect of the resonant sensor used [23 24 25]. Hence, the subtle differences which exist between sources such as cracking and fretting [13] could not be detected. Furthermore, the PH and PT data varied from zone to zone, depending on the sensor/zone separation.

Hence, no simple parameter could be found relating AE to cracking in all the zones monitored. Clearly, processing based on the use of guard sensors and a multi-sensor location system and the analysis of parametric data acquired using a resonant sensor were insufficient to identify cracking in a large region of the complex-shaped Mirage wing-spar.

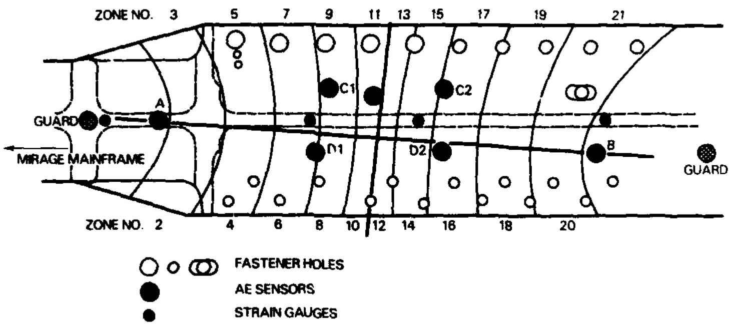

FIGURE 4 The AE sensor array (A,B,C1,C2,D1 and D2), guard sensors and zones 2-21 shown on the lower surface of the bottom flange of the Mirage wing-spar RH79[25].

Critical Assessment

While the adaptive signal processing failed to distinguish between spurious sources and AE from fatigue crack propagation in either the Mirage or Macchi aircraft applications, the Macchi test demonstrated that (i) compact AE equipment could be incorporated into an aircraft, and (ii) the continuous AE-monitoring of a large region of an aircraft in flight was feasible. The Macchi test therefore provided the necessary impetus for the further development of AE signal-processing for complex-shaped aircraft components; the Mirage test showed that advanced signal-processing would be necessary for this purpose.

THE DEVELOPMENT OF SEMI-ADAPTIVE PROCESSING

A reduction in the degree of adaptation in signal-processing should lead to greater success in the application of the processing. Hence, semi-adaptive signal-processing of AE data was developed, incorporating information on AE sources obtained during the following background research studies at ARL.

Background Research

The ARL background research included theoretical and experimental studies of sources in aircraft aluminium alloys, modelling of fatigue crack propagation during complex load-cycling, investigation of the errors in source location, sensor evaluation, the development of waveform analysis procedures and the assessment of calibration procedures for the prediction of AE features during fatigue crack propagation.

Theoretical work at ARL

Cracking of inclusions, or matrix material, in a quasi-brittle manner results in the release of energy in the form of stress waves, i.e. AE. The generation of such stress waves was studied theoretically for a straight crack in an infinite body and for an idealized model of inclusion fracture [6]. The stress waves were found to depend on the change in the crack speed at the time of generation of the waves as well as on the stress-intensity factor.

Sources in aircraft aluminium alloys A study was made of AE detected during uni-directional plastic deformation under tension or compression of aluminium alloys 2024-T351 and 2124-T351 [26]. It was concluded that the fracture of brittle inclusions is the primary source of AE detected during tensile testing. AE from slip was detected only when the aircraft alloys were heat-treated (aged) to non-standard conditions. This serves to emphasise that AE is determined not only by the applied stress system and the size and number of inclusions but also by the aged microstructure.

The work on AE in aluminium alloys was extended to include crack growth studies, conducted under constant amplitude loading conditions [7]. The results were consistent with AE associated with the fracture of brittle inclusions in the plastic zone ahead of the crack tip as the primary AE source detected. (Later theoretical work at Northwestern University [27] suggested that the likelihood of detecting AE from inclusion fracture was greater for inclusions fracturing close to the crack-tip than for inclusions fracturing elsewhere in the plastic zone.) The AE associated with inclusion fracture occurred principally at the top of the load cycle, but did not occur necessarily on every load cycle. Under the specific conditions of the test, a linear relationship was found between the average counts per load cycle and the average crack growth per load cycle for each alloy. Further AE tests were undertaken on alloy 6061-T651, chosen because its inclusions were small and the AE associated with inclusion fracture within the crack-tip plastic zone was therefore expected to be minimal, based on the results of the ARL theoretical studies [6]. AE due to crack extension alone was found to be insignificant and it was predicted to be so in all commercial aluminium-base alloys tested under similar conditions [28]. Thus, AE detected during fatigue crack growth in such alloys is likely to arise from events within the crack-tip plastic zone (and/or from crack-face rubbing), a finding corroborated by research at Royal Military College [12, 15].

More recently, fatigue cracks were grown in 2024-T351 aluminium alloy specimens cycled between fixed load limits, subjected to an overload and subsequently cycled between the original load limits [29]. During the overload, AE associated with inclusion fracture commenced at the peak cyclic load and continued until the overload peak was reached. For many cycles after the overload, the AE activity was significantly less than that prior to the application of the overload but gradually resumed it pre-overload level.

The results of other researchers (see below) suggest that AE from spurious sources could occur at a range of different load-cycle positions, depending on factors like the loading conditions used (load limits, non-axiality in load application, etc.), the specimen configuration and microstructural considerations. For example, AE from fretting of a bolt in a hole was observed on negative load gradients for fixed load limit cycling of bolted plates [13], and at other load-cycle positions for misaligned specimens. AE from crack-face rubbing has usually been observed on positive load gradients, occurring both below the mean load and repetitively for many hundreds of cycles before ceasing abruptly [30, 31]. Results of a recent study [10] suggest that AE from crack-face rubbing could also occur at the top of a load cycle under certain experimental conditions. However, the results of this study were difficult to evaluate, because of the possible effects of an inhomogeneous size distribution of inclusions on the AE detected during a limited number of load cycles.

Sensors In the course of a sensor evaluation program [32], it was established that detailed determination of AE source characteristics can only be achieved if AE measurements are made using a wide-band sensor rather than a resonant sensor (as in the earlier Macchi and Mirage aircraft studies). Quantitative analysis requires additional sensor characteristics.

AE source-location A comparison [33] between results obtained from a state-of-the-art AE source location system (with a four-sensor array) and computer-modelled results showed that accurate location of remote AE sources is difficult even in a simple structure (i.e. a flat plate). Near the array sensors, the location equations yielded ambiguous or imaginary solutions and outside the array accuracies diminished rapidly. Experimentally, problems were experienced in setting detection levels, with different levels resulting in the detection of different plate modes (Table I). Hence, even greater problems could be expected if source-location techniques were applied to more complex-shaped structures.

TABLE I Overall means of variances of Δ T (arrival times) for waves generated using range of driver levels and detected by an array sensor 600 mm from the pulser but on the same surface of a 6 mm thick aluminium plate. Mean time positions of individual distributions of ΔT and percentages of measurements represented by them are also given [33].

Pulse drive level	Mean & var. of ΔT (μs)	Mean ΔT's in μs (and percentage of measurements represented) of individual distributions			
Max	81.56 + 0.50	81.56	(100%)		
1	82.19 + 1.38	81.60	(82.9%);	85.04	(17.1%)
2	84.32 + 1.52	81.58	(20.7%);	85.08	(78.9%)
4	81.89 + 0.68	81.79	(96.7%);		
5	82.83 + 1.57	81.81	(68.9%)	85.09	(31.1%)
6	83.50 + 0.52	83.49	(100%);		
8	84.11 + 1.42	83.15	(59.9%);	85.70	(38.8%)
Min	87.08 + 0.33	87.08	(100%)		

Waveform analysis to distinguish between sources Many useful features for distinguishing between sources can be obtained from accurately recorded AE waveforms [9 13 25 34]. At ARL a computer program was used to extract features from digitized waveforms and to provide a means for applying acceptance/rejection criteria (based on these features) to distinguish between sources [8]. The program allowed examination of the following features:

1. Saturation data: a waveform was rejected if it was clipped.
2. Rise-time and duration: minimum acceptable values were set.
3. Shape factors in the time domain: mean, standard deviation, skewness and kurtosis (α_4) were calculated.
4. The autocorrelation function C_j (j is the numeric separation between two arbitrary points in the digitized waveform): acceptance/rejection criteria were determined based on $dC_j/dj=0$.
5. Spectral information: Fourier transforms were obtained and power ratios for five frequency bands compared.

Features extracted from a set of AE waveforms depend not only on the type of source but also on several other factors, viz. (i) the source location, (ii) the sensor used to obtain the waveforms, (iii) the test-piece, and (iv) the position of the sensor on the test-piece. Hence, the features found to distinguish between AE from different sources in a particular application cannot simply be used to identify the emission from such sources in an arbitrary application. However, if a suitable source can be selected to simulate a defect-related source of interest, then the simulated source can be used to predict the features appropriate to different combinations of test-piece, sensor and source location. Acceptance/rejection criteria can then be formulated from these features and applied to AE waveforms detected during structural monitoring.

The above procedure was successfully used in a research laboratory application to distinguish between AE waveforms from inclusion fracture and from extraneous sources including gas flow, electromagnetic interference, mechanical noise and transient electronic noise [8]. The features used to formulate the acceptance/rejection criteria were rise-time, duration and the value of j for the first minimum in C_j, which were obtained using Pentel lead fracture [35] as a source simulating AE associated with inclusion fracture (Table II). The procedure was also used to distinguish between different locations of the simulated source. Hence, possible discrepancies in the (source) location of cracking by sensor arrays could be checked by comparing measured features and features predicted for a given location using a simulated source.

TABLE II A selection of features, α_4 C_1 and j (see background studies), extracted from waveforms from several AE sources. The percentage of waveforms meeting minimum risetime and duration criteria [8] are shown. The combination of features of the autocorrelation function and risetime/duration of AE waveforms enabled extraneous and damage-related sources to be distinguished. In addition, the Pentel source gave similar features to AE from inclusion fracture, showing its usefulness as a simulated source.

Source type	α_4	C_1	j	%
Extraneous:				
Gas flow	2.72–3.33	0.99	34–38	0
Electromagnetic interference	3.32–5.83	-0.12–0.17	1	60
Mechanical noise	2.96–4.79	0.98–0.99	33–39	100
Transient electronic noise	3.42–25.43	0.68–0.87	5	0
Damage-related:				
Inclusion fracture	1.66–5.63	0.84–0.91	5–8	100
Simulated:				
Pencil lead fracture	5.06–7.05	0.90–0.94	7–8	100

Load dependence of AE from crack growth The earlier AE results obtained during the application of a single overload amidst otherwise constant amplitude load cycling of aircraft aluminium alloys indicated that the load dependence of AE associated with crack propagation could be a useful feature for source identification. Therefore, an attempt was made to extrapolate from these earlier AE results to model the likely load dependence of AE due to cracking during the more random loading typical of aircraft applications. The model [4] was based on well-established results on the *effects of* the amplitude and *frequency of* loading on the likelihood of fatigue crack propagation. Analogously to the load dependence of AE during application of a single overload, the model proposed that, on any given cycle during random load-cycling, AE associated with fatigue crack propagation could occur in a load range defined by a positive load gradient between a lower load level (denoted ML) and the top of the cycle.

The main steps in calculating ML, which could vary from cycle to cycle (depending on loading history), were as follows:

(i) An arbitrary constant amplitude loading level (LC) was selected and initially set as ML (Fig.5(a)).
(ii) The first load cycle having an amplitude above this level was treated as a dominating overload whose amplitude was defined as LO, with AE associated with fatigue crack propagation being possible between ML and LO (Fig.5(a)).
(iii) ML was set to LO immediately after the overload LO but ML was then assumed to decrease exponentially during subsequent cycling (corresponding to the diminishing effect of the overload) according to the formula LO*exp(-(n*LC/(T*LO)), where T was a set decay constant and n was the number of cycles after application of the dominating overload LO.
(iv) For each cycle n during this subsequent cycling, AE associated with crack propagation was assumed to be possible on a positive load gradient from the stage at which the load level again exceeded ML (corresponding to n) until a peak load was reached. The peak load was treated as an additional (dominating) overload if its amplitude exceeded LC (Fig.5(b)). The amplitude of this additional overload was then set as LO and (iii) recalculated on this basis for the cycles following the second overload. (Step (iv) was applied repetitively (Fig.5(c)).)

This calculation would result in the exclusion of any AE associated with fatigue crack propagation at the tops of a number of cycles following an overload (Fig.5) but the source would be more likely to occur in the load range between ML and the top of the cycle (denoted range 1).

The relationship between AE activity and load for spurious sources could be expected to differ from that for fatigue crack propagation. Hence, three additional loading ranges were defined wherein AE activity could be compared with range 1 activity. For each cycle dominated by an overload LO, the ranges were set relative to the crack opening load level (i.e. > 0.6*LO) and crack closing level (i.e. < 0.4*LO) for the overload. The ranges, labelled 2-4, were:

(2) decreasing load above 0.6*LO
(3) decreasing load below 0.4*LO
(4) increasing load above 0.6*LO

A computer program was written to enable comparison of the AE in the four loading ranges and the possible distinction of AE sources on this basis.

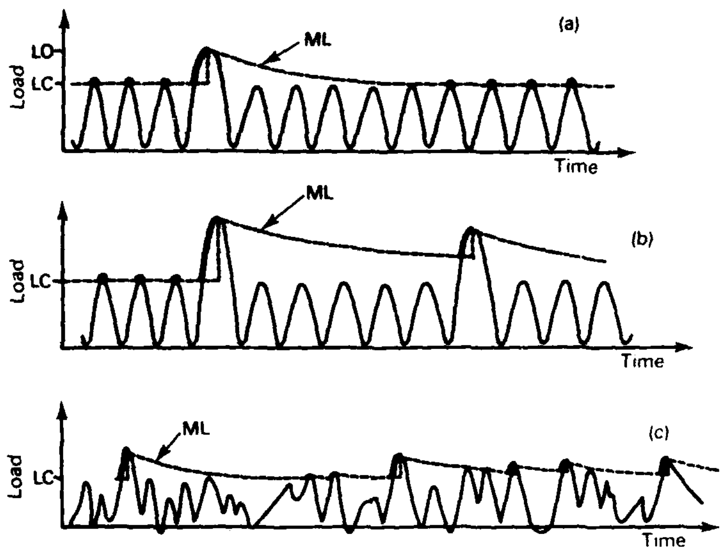

FIGURE 5 Regions on the loading curve where AE from fatigue crack propagation could occur are shown as heavy lines and ML (the lower level at which AE from fatigue crack propagation could occur on a given cycle) is shown dashed (a decay constant of 10 cycles is assumed):

(a) application of single overload (LO) amidst otherwise constant amplitude (LC) load cycling for LO=1.5*LC
(b) application of a second overload
(c) random load cycling typical of aircraft applications.

Semi-adaptive Processing

A procedure for semi-adaptive processing of AE data was developed at ARL for AE-monitoring of complex-shaped aircraft structures based upon the AE results obtained, the computer programs written and the procedures established in the background research above. Two types of semi-adaptive processing were proposed. Each type was based (to a greater or lesser extent) on the use of limited a priori information on AE sources. The first type incorporated known information in the processing of AE waveforms from which a wide variety of features could be extracted. The second, more adaptive (or empirical) processing was based on the extrapolation of the known data on the load dependence of AE events and was developed with the aim of simplifying future instrumentation.

The semi-adaptive processing of AE waveforms [2, 5] involved the identification of AE due to fatigue crack propagation by a comparison between (i) features extracted by pattern-recognition analysis of emission detected during aircraft-monitoring, and (ii) features predicted for AE due to fatigue crack propagation. Feature prediction was based on (i) the known and usable information on AE sources in complex-shaped structures, and (ii) wave propagation characteristics, determined from calibration studies using a Pentel-lead source known to simulate closely AE from fatigue cracking (see earlier). Risetime and autocorrelation function characteristics (extracted from AE waveforms, acquired using a wide-band sensor so that sensor characteristics do not dominate the pattern recognition analysis) and known data on the position on the load cycle of AE event occurrence where used as criteria to select AE from fatigue-cracking.

The more empirical processing [4] involved a comparison between the observed load dependence of AE events and the behaviour predicted (by extrapolating from the known data) for AE due to fatigue crack propagation during random load-cycling. Cracking indications were obtained by comparing the AE activity in the likely fatigue crack propagation range and in three other ranges (described above) in the loading curve.

Further details on the semi-adaptive processing are given in the next section in respect to its application to the problem of identifying and locating AE from fatigue crack propagation in Mirage aircraft.

SEMI-ADAPTIVE PROCESSING OF AE FROM A MIRAGE AIRCRAFT

Overview of Experimental Details

The equipment and procedure for AE monitoring of the full-scale fatigue test of a Mirage aircraft were modified to allow implementation of semi-adaptive processing [2, 5, 36]. The modified data acquisition system contained a sensor array and guard sensors (as in the AE monitoring of wing RH79 described earlier) but also included a wide-band sensor for waveform acquisition and enabled the measurement of the load-cycle dependence of AE events. In addition, the procedure included calibration studies using a simulated AE source. A second Mirage wing (RH56) was instrumented with the modified AE equipment and the slow fatigue crack propagation expected in several fatigue-critical holes in the main wing-spar of the aircraft was monitored. The complex-shaped wing-spar was made from a relatively "dirty" aluminium alloy (AU4SG), which usually contains many large, brittle inclusions. Hence, AE associated with the fracture of inclusions was the likely damage-related AE source to be distinguished from the spurious sources present during the fatigue testing.

The fatigue-critical region monitored in the bottom flange of the main wing-spar of wing RH56 was smaller than the region monitored in wing RH79. The holes monitored comprised the twelve bolt-holes (containing interference-fit bolts) closest to the aircraft's mainframe on the forward side of the flange, the two empty single-leg-anchor-nut (SLAN) rivet holes on the rear side of the flange, and the eight bolt holes (containing close-tolerance bolts) nearest to the mainframe on the rear side of the flange (as with wing RH79, this monitored region is referred to as the critical part of the flange). A refurbishment programme used on wing RH56 had resulted in interference-fit, stainless steel bushes being inserted in the five rear bolt holes closest to the mainframe [37], while the first seven rear bolts attached not only the wing-skin but also a metal-patch repair to the skin; also, a boron-fibre patch repair had been adhesively bonded to part of the wing-skin (Fig.6).

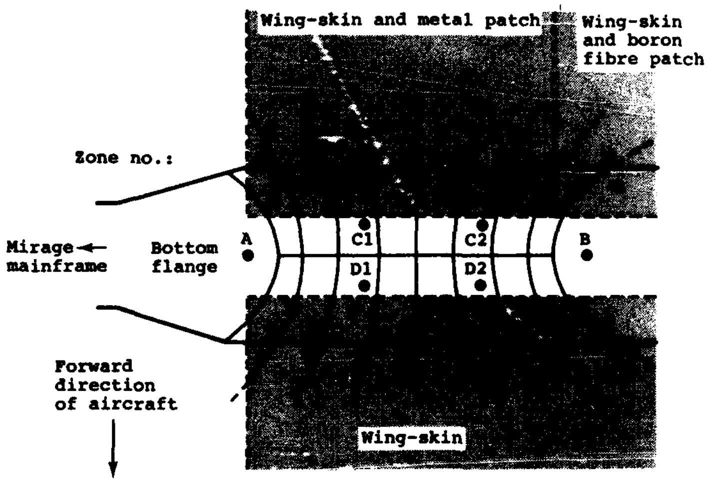

FIGURE 6 Schematic view of the lower surface of Mirage wing RH56[5] showing
(i) part of the bottom flange, wing-skins and repair patches;
(ii) the location of the sensor array (A, B, C1, C2, D1 and D2) used for zone assignment;
(iii) the bolt holes and empty SLAN rivet holes;
(iv) the AE zones 4–19.

Complete details of the modified AE data acquisition system have been given previously [4, 5]. The system comprised a six-sensor array and nine guard sensors to minimize the detection of sources extraneous to the critical part of the bottom flange and to locate sources within sixteen zones within the critical part of the flange (Figs. 6&7).

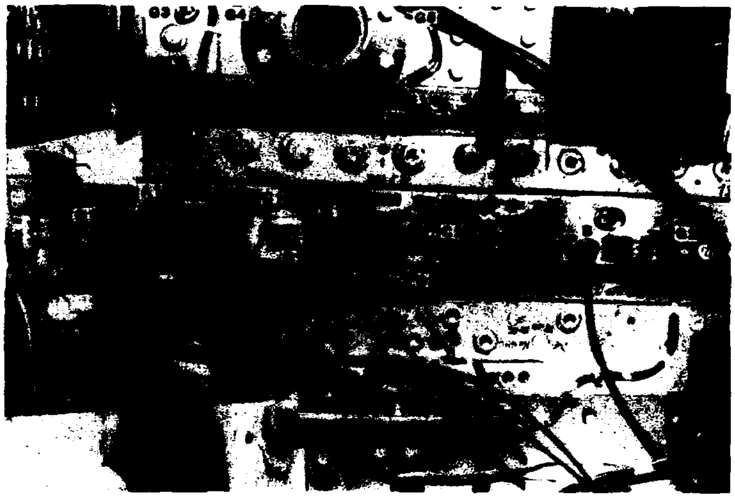

FIGURE 7 Location on lower surface of Mirage wing RH56 of guard sensors G1 and G2 on the bottom flange of the wing-spar, guard sensors G3, G4 and G5 on a patch on the wing-skin, waveform sensors W (used earlier for adaptive monitoring), W1 and A1, and the sensor array[5].

The following data were obtained during fatigue testing:

(i) Continuous collection of spar strain-gauge information, the pulse height and peak time of AE events (detected at a resonant sensor located at A (Fig. 7), the zone number and the time in seconds relative to the start of the test.

(ii) Acquisition of AE waveforms for a short period; the waveforms were acquired following 8200 simulated flights in the fatigue test, and were detected using wide-band sensors located at either A1 or W1 (Fig. 7) (the waveforms were recorded with corresponding zoning information, the time and strain gauge data).

(iii) Acquisition of additional waveforms in calibration studies, using the fracture of Pentel lead to simulate AE associated with inclusion fracture. The zone assignment for each simulated source location was recorded with each AE waveform.

AE Waveform Analysis

Procedure Zoning data from the Pentel lead calibration studies above were used to assess the effectiveness of the guard sensors and the accuracy of source-location by the sensor array.

Two criteria were formulated from autocorrelation function and risetime characteristics of the Pentel lead waveforms in order to reject AE waveforms from spurious sources during fatigue testing on the basis of features related to wave propagation. Criterion (i) specified features of Pentel lead fractures generated anywhere within the critical part of the flange; criterion (ii) specified the features obtained from Pentel lead fractures at all the holes in the critical part of the flange. An additional criterion (denoted (iii)), based on a usable source-related feature of AE associated with inclusion fracture was also specified: AE waveforms were defined as having the load-dependence of a damage-related source if they occurred intermittently at the tops of load-cycles. (AE associated with inclusion fracture could also be expected to occur on a positive load gradient (see background studies).)

A comparison between the features extracted from AE waveforms detected during fatigue-testing and the features predicted for AE from fatigue crack propagation in the critical part of the bottom flange was made in three steps, with each succeeding step involving examination of more precise features. The first step involved applying the above criterion (i) to the AE waveforms detected during fatigue testing to eliminate AE from sources extraneous to the bottom flange. The second step involved applying criteria (ii) and (iii), in order to determine any AE-based cracking indications in the flange, without (at this stage) attempting to obtain the actual location of the cracking. The third step involved determining the location of the cracking by a direct comparison between features of those AE waveforms attributed in step 2 to fatigue crack propagation and the features of Pentel lead fractures obtained at specific holes.

AE results for zones 10 and 11 The application of semi-adaptive processing to AE waveforms to eliminate AE from spurious sources and to detect fatigue crack propagation can be demonstrated by detailed examination of AE waveforms assigned to zones 10 and 11. (The analysis is representative of that involved for any of the zones monitored (see later).)

The tests using Pentel lead AE events showed that the accuracy of the source location system varied with the position of the simulated source: in particular, events generated towards the mid-point of the sensors A and B were more accurately located than events generated near the sensors themselves [16]. For example, events generated at various locations around the zone 11 hole were usually assigned to zone 11 (and zone 10 events to zone 10), whereas events generated around the zone 9 hole were assigned to either zone 9 or zone 11. Hence, after fatigue-cracking had been identified and assigned to zones, it was necessary to check for location discrepancies.

Criterion (i) was specified from the Pentel results as follows: an AE waveform was identified as originating within the critical part of the bottom flange if its risetime was less than 100 μs and the first minimuim in its autocorrelation function occurred at a lag of 21 or less. 77% of the AE waveforms assigned to zone 10, and 25% of those assigned to zone 11, failed to meet this criterion. Hence, the guard system was clearly satisfactory for zone 11, but allowed significant AE from an extraneous source to be located in zone 10. Based on approximate calculations, this extraneous source was associated with an unguarded fairing attachment extending from the mainframe to the nearby wing-skin.

Criterion (ii) was specified from the Pentel lead results as follows: an AE waveform was defined as originating at any of the holes in the critical part of the flange if it exhibited a risetime of less than 50 μs and first minimum in its autocorrelation function at the lag of 21 or less. AE waveforms satisfying criteria (ii) and (iii) were assigned to zone 11 but not to zone 10 during fatigue testing [5]. Hence, at this stage in processing, indications of cracking in the spar were obtained for AE waveforms assigned to zone 11.

The indications of cracking for AE waveforms assigned to zone 11 could have been due to cracking in either the zone 9 or the zone 11 hole, given the assignment (above) of Pentel lead events by the location system. Hence, the final step in processing involved checking the location of the zone 11 waveforms satisfying criterion (ii) by a comparison between their features and the Pentel lead features for the zone 9 and 11 holes. It was found that, for both waveform sensor locations used, the zone 11 waveforms exhibited features corresponding to Pentel events at the zone 9, and not the zone 11 hole. Calculations based on the spar geometry confirmed that zone 9 events would be assigned to zone 11 when first-arrival waves were longitudinal, rather than Rayleigh, and were of sufficient amplitude to be detected by the sensor array. Hence, the AE waveform processing gave a cracking indication in the zone 9 hole.

AE in other zones Zones 5 and 9 were the only other zones to which waveforms meeting criteria (ii) and (iii) were assigned during fatigue testing [5]. A detailed comparison of the features of these zone 5 and 9 waveforms with Pentel lead results indicated that these waveforms were due to cracking in the zone 5 holes.

Comparison of AE and fractographic results Quantitative fractography [16] following completion of the full-scale fatigue testing of Mirage wing RH56 showed that several large cracks had propagated in the wing-spar at the zone 5 and zone 9 holes during the fatigue test (Fig. 8); cracking from zone 5 caused final failure of the wing. The holes in zones 5 and 9 were the only holes having propagating cracks greater than 0.3mm in depth during the waveform acquisition. Thus, the cracking indications from the semi-adaptive processing of AE waveforms were confirmed.

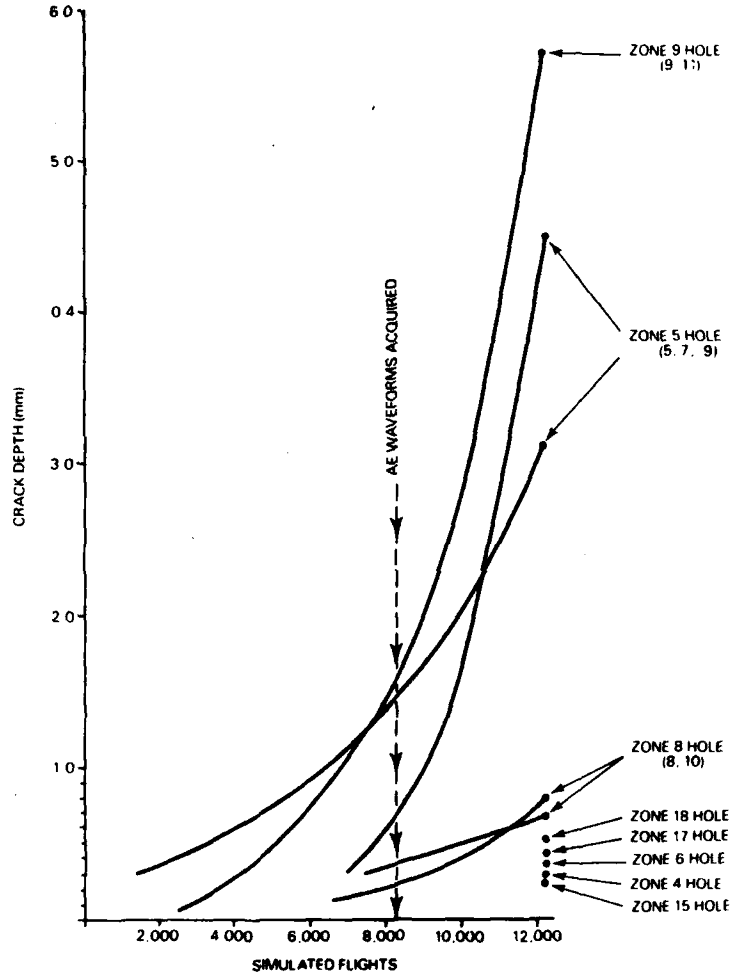

FIGURE 8 Crack depths in wing RH56 as the fatigue test progressed[4,38]. Predicted zone locations of larger cracks are given in brackets. The start of AE waveform acquisition (undertaken for approximately 200 flights) is also shown.

Analysis of Load Cycle Dependence of AE Events

Procedure The detailed loading information required for the data analysis was obtained by reconstructing the load/time curve for the Mirage testing from the strain and time data recorded for each AE event. Regions on the load/time curve corresponding to the ranges 1-4 were determined (Fig.9), with load range 1 being calculated using empirically selected constants T=10 cycles (corresponding to ML being set at about 90% of the peak load for constant amplitude load cycling in agreement with the results of background AE studies) and LC=3.2 g (i.e. close to half the maximum load level of 7.5 g reached in the full-scale fatigue test). As the fatigue test progressed, the distribution of AE events among the four ranges was compared for each zone; cracking indications were based on relatively high activity in range 1.

Application of detailed load/time analysis For each zone, Fig. 10 shows the distribution of AE events (among the four load ranges) just prior to the failure of Mirage wing RH56. Zones 9, 10 and 11 were the only zones in which the distributions were clearly consistent with the expected behaviour of AE from fatigue crack propagation; such cracking indications were obtained in zones 9, 10 and 11 throughout the AE-monitoring of the fatigue test [4]. However, the AE cracking indications were inconsistent with fractographic results obtained on completion of the fatigue test (Fig.8) - as the test progressed, major cracks in the spar propagated rapidly in the holes in zones 5 and 9 (as discussed above) whereas late in testing small cracks developed in the zone 8 hole.

The results of the earlier AE waveform processing showed that inaccuracies could be expected in the zone location of AE events. Correction of the AE data from the load analysis for this factor allowed a good agreement to be obtained between the AE cracking indications in zones 9 and 11 and the large cracks present in zones 5 and 9 (Fig. 8). The similar levels of the AE cracking indications obtained in the zones 9, 10 and 11 (Fig. 10) suggested that the AE activity in zone 10 was also due to a large, rapidly propagating crack. Correction of the AE data in zone 10 for possible mis-zoning showed that the substantial cracking indications obtained in zone 10 throughout the Mirage test could have been due to sources in either the zone 8 or zone 10 holes (or, as suggested by the waveform analysis, to unguarded extraneous sources). However, no cracks were measurable in the zone 8 and zone 10 holes early in the test (Fig. 8). In addition, no cracks were measurable in the zone 10 hole and only small cracks were found in the zone 8 hole late in the test. Hence, the zone 10 results obtained from the AE load analysis have to be classified as unreliable.

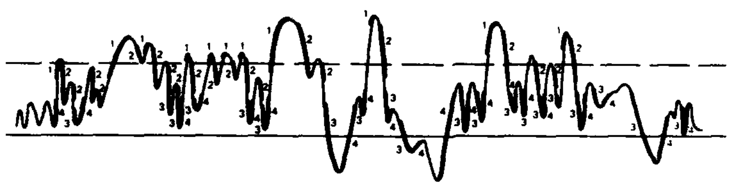

FIGURE 9 A typical load sequence used in the Mirage test, showing regions on the loading curve corresponding to ranges 1 to 4 in which relative AE activity was compared[4].

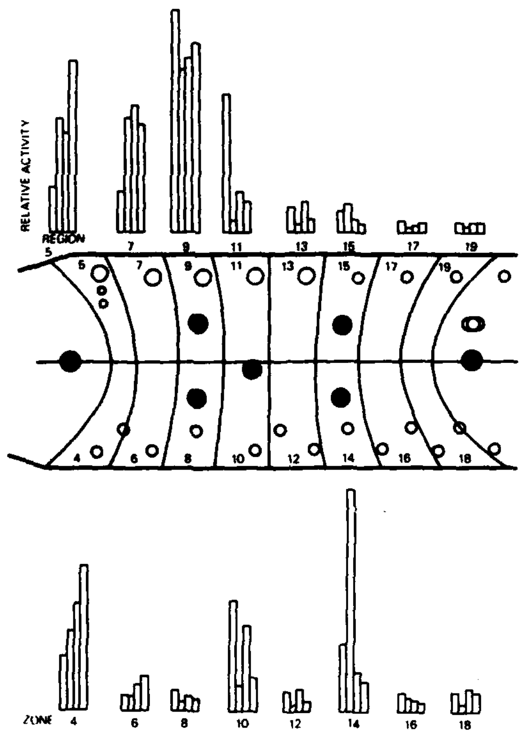

FIGURE 10 Relative AE activities in the 16 zones in wing RH56 (towards the end of the fatigue test). The distribution of AE events among the four load ranges is shown for each zone (ranges 1–4 are given from left to right respectively)[4].

In summary, the load analysis of AE data was insufficient to positively identify cracking when used in isolation. When used with calibration data, the sensitivity of the load analysis to cracking was similar to that of the waveform analysis, resulting in the detection of all cracks greater than 0.3 mm in depth*. However, the load analysis was less accurate than the waveform-analysis, and only gave cracking indications to within one of several zones. In addition, the technique was less reliable than the waveform analysis, resulting in inconsistencies in the data and some false cracking indications. Measurements of additional AE features, such as those used in the waveform-processing, would be required to resolve these apparent inconsistencies (although the use of more guard sensors would be a step towards removing false cracking indications). Additional features would also be required if more accurate location of cracking indications were required.

CONCLUSIONS AND FACTORS AFFECTING FUTURE AE MONITORING

It can be concluded from the Mirage study above that semi-adaptive processing of AE waveforms provides a valuable and reliable method for identifying AE due to fatigue crack propagation, even when many spurious sources are present. Promising results were also obtained using more empirical processing (based on extrapolation from some of the known information on the load cycle dependence of AE events) although some inconsistencies in cracking indications were obtained. In addition, the limitations of applying (i) guard sensors to eliminate extraneous sources, and (ii) sensor arrays for source location have been demonstrated.

The ARL research has resulted in the development of an extensive science-base for future AE studies on aircraft. Ideally, future AE-monitoring to identify and locate fatigue crack propagation in complex-shaped aircraft components would involve (i) preliminary processing using many guard sensors and an extensive sensor array, (ii) semi-adaptive processing with the minimum degree of adaptation possible, and (iii) real-time assessment of defect criticality. In practice, the choice of processing will require several factors to be considered and balanced, including the reliability required of the inspection (which will determine the level of adaptation necessary), the equipment available for the AE measurements, the resources available for purchase of new equipment, space limitations in the aircraft for installation of AE equipment, the need (and the resources available) for additional background studies and the overall aim of undertaking AE monitoring. The remainder of this discussion will briefly consider the implications of some of these factors.

Reliability of Processing

Clearly, greater reliability in applying AE to identify and locate cracking is related to lowering the degree of adaptation in AE processing: greater accuracy was achieved from AE waveform processing (to wing RH56) than from the more adaptive analysis of the load-dependence of AE events (the adaptive processing on wing RH79 could be classified as unreliable). Hence, the reliability required would be a major factor (along with equipment availability) in choosing between AE waveform processing and load analysis in a future application. Consideration could also be given to increasing reliability by undertaking additional background studies to increase the usable information on AE source characteristics in complex-shaped structures (see later); the degree of adaptation could then be reduced from that applicable in the Mirage study.

Equipment

An improved capability for rejecting extraneous sources could be gained by the application of more guard sensors than used in the Mirage test. In addition, the use of a more extensive sensor array could enable more accurate zone location of fatigue crack propagation, provided that (i) a single wave speed could be assumed for time-of-flight calculations, or (ii) corrections could be made for multiple wave modes by subsequent application of semi-adaptive processing. However, the major penalty from applying more extensive arrays, etc., is the probable lowering of the AE data acquisition rate, as time-consuming computation is involved if complicated algorithms are used for on-line time-of-flight analysis.

The progress which continues to be made in all aspects of AE instrumentation (including its miniaturization [39]) should greatly facilitate future in-flight monitoring by AE. The current NBS research [40] should lead to a range of useful sensors for non-adaptive measurements (which will allow very accurate source location and identification), while the existence of sensors suitable for permanent mounting in an aircraft has been demonstrated in this paper. In addition, the future, in-flight utilization of powerful semi-adaptive processing, such as described herein, will be greatly assisted by recent advances in dedicated microprocessors and extended computer memories. In past years, equipment restrictions would have resulted in the adoption of processing based on some form of load analysis (together with limited analysis of parametric AE data) rather than the more cumbersome acquisition of AE waveforms (and subsequent laboratory analysis of data). However, the improvements in digital electronics will enable the direct in-flight application of acceptance/rejection criteria (whether based on risetimes, lags, load-dependence or more fundamental features) for distinguishing between AE sources. For example, EPROM'S are now available with storage up to 4 Mbit [41], and DRAM-CMOS dynamic random access memory are also available to 4 Mbit. The use of existing on-board computer facilities, which would enable real-time defect assessment by AE, is also a possibility.

Additional Background Studies

The semi-adaptive processing of AE waveforms from the Mirage wing enabled the correct identification of cracking in the wing-spar by isolating AE events with specific features. However, these features were not shown to be unique to fatigue cracking due to insufficient information on all the possible AE sources in the Mirage test. Additional background studies could be undertaken to increase knowledge of the characteristics of likely spurious sources in aircraft applications. However, the cost-effectiveness of such studies could be questioned, e.g. there is no need to determine unique features to distinguish between AE from crack propagation and crack face rubbing as crack face rubbing is itself a useful crack indicator [42]. In addition, the benefits of further studies would be marginal for AE-monitoring of complex-shaped structures as only limited information would be usable.

The semi-adaptive processing used in the present paper has been directed towards AE-monitoring of aircraft aluminium alloys but the procedures are generally applicable to other aircraft materials. While many source-related features are known in composite, ceramic and other metallic aircraft materials [9, 43], additional studies on the load dependence of these sources would be of value for future AE monitoring. Moreover, additional studies of features such as the directivity patterns of both spurious and damage-related sources would be of benefit in the AE-monitoring of components with simpler shapes than the Mirage wing. In such applications, non-adaptive processing could be feasible and a unique inversion of AE data possible. Practical implementation of an accurate source location system such as developed at Harwell [18] could be useful in such cases; the system could even be used to characterize better AE associated with inclusion fracture during fatigue crack propagation by establishing the location(s) of the inclusion fracture within the plastic zone.

AE and Airworthiness

The ARL research has demonstrated the feasibility of in-flight AE monitoring; the ability of the technique to identify crack growth under laboratory and full-scale fatigue test conditions has been established and the feasibility of in-flight AE measurements has been demonstrated. Real-time AE-monitoring also seems feasible in the near future given the rapid advances being made in instrumentation.

In airworthiness terms, the capability of AE for identifying and locating growing cracks in complex-shaped components has been established. However, an examination of the procedures required for successful AE-monitoring shows that AE is a specialist technique which is unlikely to be used routinely to determine structural integrity. The benefits in applying AE are likely to be found when costs, delays and even damage associated with the regular disassembly of an aircraft for more conventional NDI become prohibitive. Moreover, the AE technique now offers a solution to many of the inspection problems which cannot be tackled using conventional techniques.

ACKNOWLEDGEMENTS

The authors wish to acknowledge the significant contribution made by other ARL staff (both past and present) to the research described in this paper. R.A. Coyle undertook much of the computer programming for the analysis of the Mirage and Macchi AE data. Dr. G.G. Martin (now at ATTAR) and S.R. Lamb made major contributions to the Macchi project. The assistance of B.C. Bishop, R.A. Pell and N.T. Goldsmith with metallography is also appreciated. The interest shown by Dr. F.P. Bullen and the contributions made by Dr. L.R.F. Rose and S.McK. Cousland to the background research are also acknowledged.

The Macchi and Mirage projects were only possible due to the sophisticated AE systems developed by Battelle Pacific Northwest Laboratories - particular thanks are due to P.H. Hutton (Project Manager), Dr. D.K. Lemon and J.R. Scorpik for their efforts.

The support and encouragement provided by the Royal Australian Air Force and the staff (particularly Dr. H. Boesch) at the Swiss Federal Aircraft Factory, Emmen, are also gratefully acknowledged.

REFERENCES

1. C.B. Scruby, J. Phys. E, 20:946-953 (1987).
2. C.M. Scala, Review of Progress in Quantitative Nondestructive Evaluation, Vol. 6, Ed. D.O. Thompson and D.E. Chimenti, Plenum Press, New York, pp. 361-369 (1987).
3. I.G. Scott, Proc. 13th Symp. on Nondestructive Evaluation, Ed. B.E. Leonard, NTIAC, pp. 210-219 (1981).
4. S.J. Bowles, NDT International (in preparation, 1987).
5. C.M. Scala, J. Acoust. Emission (in press, 1987).
6. L.R.F. Rose, Int. J. Fract., 17:45-60 (1981).
7. C.M. Scala and S.McK. Cousland, Mater. Sci. Engng., 61:211-218 (1983).
8. C.M. Scala and R.A. Coyle, NDT International, 16:339-343 (1983).
9. C.B. Scruby, Research Techniques in Nondestructive Testing, Vol. 8, Ed. R.S. Sharpe, Academic Press, London, pp. 141-210 (1985).
10. G. Weatherly, J.M. Titchmarsh and C.B. Scruby, Mater. Sci. Technol., 2:374-385 (1986).
11. S.L. McBride and J.W. Maclachlan, J. Acoust. Emission, 1:223-228 (1982).
12. S.L. McBride, J.W. Machlachlan and B.P. Paradis, J. Nondestr. Evaln., 2:35-41 (1981).
13. L.J. Graham and R.K. Elsley, J. Acoust. Emission, 2:47-55 (1983).
14. J.M. Richardson, R.K. Elsley and L.J. Graham, Pattern Recognition Letts., 2:387-394 (1984).
15. S.L. McBride and J.L. Harvey, Review of Progress in Quantitative Nondestructive Evaluation, Vol. 6, Ed. D.O. Thompson and D.E. Chimenti, Plenum Press, New York, pp. 353-360 (1987).
16. C.R. Horak and A.F. Weyhreter, Mater. Evaln. 35:59-63 (1977).
17. H.J. Rindorf, Bruel & Kjaer Tech. Rev., 2:3-42 (1981).
18. C.B. Scruby, J. Acoust. Emission, 4:9-42 (1985).
19. D.R. Hay, R.W.Y. Chan, D. Sharp and K.J. Siddiqui, J. Acoust. Emission, 3:118-129 (1984).
20. P.H. Hutton, D.K. Lemon, R.K. Melton and P.G. Doctor, Review of Progress in Quantitative Nondestructive Evaluation, Vol. 1, Ed. D.O. Thompson and D.E. Chimenti, Plenum Press, New York, pp. 459-462 (1982).
21. S.R. Lamb, Aircraft Materials Tech. Memo 393, Aeronautical Research Laboratories, Melbourne (1987).
22. I.G. Scott Proc. 4th Pan Pacific Conf. on Nondestructive Testing, Paper AE4, Australian Institute for Nondestructive Testing, Sydney (1983).
23. S.J. Bowles, Proc. 4th Pan Pacific Conf. on Nondestructive Testing, Paper AE3, Australian Institute for Nondestructive Testing, Sydney (1983).
24. S.J. Bowles, Abstr. in Proc. New Zealand Nondestructive Testing Assoc. 10th Annual Symposium, Wellington (1986).
25. C.M. Scala, R.A. Coyle and S.J. Bowles, Review of Progress in Quantitative Nondestructive Evaluation, Vol. 4B, Ed. D.O. Thompson and D.E. Chimenti, Plenum Press, New York, pp. 709-718 (1985).
26. S.McK. Cousland and C.M. Scala, Mater. Sci. Engng., 57:23-29 (1983).
27. J.D. Achenbach, K.I. Hirashima and K. Ohno, J. Sound and Vibration, 89:523-532 (1983).
23. S.McK. Cousland and C.M. Scala, J. Mater. Sci. Letts., 3:263-270 (1984).
29. C.M. Scala and S.McK. Cousland, Mater. Sci. Engng., 75:83-88 (1985).
30. T.C. Lindley, I.G. Palmer and C.E. Richards, Mater. Sci. Engng., 32:1-15 (1978).

31. C.J. Kim and J. Weertman, Microstructural Characterization of Materials by Non-microscopical Techniques, Ed. N. Hessel Anderson et al., Riso National Laboratory, Denmark, pp. 349-353 (1984).
32. C.M. Scala, J. Acoust. Emission, 2:275-279 (1983).
33. J.F. Nankivell, Nondestructive Testing Australia, 21:9-11 (1984).
34. D.M. Eagle, C.A. Tatro and A.E. Brown, Mater. Evaln., 39:1037-1044 (1981).
35. N.N. Hsu, U.S. Patent 4018084 assigned to Lockheed Aircraft Corp. (1975).
36. C.M. Scala, Materials Tech. Memo 388, Aeronautical Research Laboratories, Melbourne (1984).
37. J.Y. Mann, A.S. Machin and W.F. Lupson, Structures Report 398, Aeronautical Research Laboratories, Melbourne (1984).
38. R.A. Pell, Failure Analysis Report M1/86/RAP, Aeronautical Research Laboratories, Melbourne (1986).
39. S.L. McBride, private communication (1987).
40. T.M. Proctor, J. Acoust. Emission, 5:134-142 (1986).
41. "Toshiba reveals its memories" Electronics and Power, p. 297, May (1987).
42. S.L. McBride and J.W. Maclachlan, J. Acoust. Emission, 3:1-9 (1984).
43. I.G. Scott and C.M. Scala, Composite Materials for Aircraft Structures, Ed. B.C. Hoskin and A.A. Baker, AIAA Education Series, New York, pp. 175-192 (1986).

DISTRIBUTION

AUSTRALIA

Department of Defence

Defence Central

Chief Defence Scientist
Assist Chief Defence Scientist, Operations (shared copy)
Assist Chief Defence Scientist, Policy (shared copy)
Director, Departmental Publications
Counsellor, Defence Science (London) (Doc Data Sheet Only)
Counsellor, Defence Science (Washington) (Doc Data Sheet Only)
S.A. to Thailand MRD (Doc Data Sheet Only)
S.A. to the DRC (Kuala Lumpur) (Doc Data Sheet Only)
OIC TRS, Defence Central Library
Document Exchange Centre, DISB (18 copies)
Joint Intelligence Organisation
Librarian H Block, Victoria Barracks, Melbourne
Director General - Army Development (NSO) (4 copies)
Defence Industry and Materiel Policy, FAS

Aeronautical Research Laboratory

Director
Library
Superintendent - Aircraft Materials
Divisional File - Aircraft Materials
Authors: C.M. Scala
S.J. Bowles
I.G. Scott
J. Grandage
G. Clark
D. Arnott
S. Lamb

Materials Research Laboratory

Director/Library

Defence Science & Technology Organisation - Salisbury

Library

WSRL

Maritime Systems Division (Sydney)

Navy Office

Navy Scientific Adviser

Army Office

Scientific Adviser - Army

Air Force Office

Air Force Scientific Adviser
Aircraft Research and Development Unit
  Library
Technical Division Library
Director General Aircraft Engineering - Air Force
Director General Operational Requirements - Air Force
HQ Operational Command (SMAINTSO)
HQ Support Command (SENGSO)
HQ Support Command (CLOG)
AIRENG 5B
C. Bott DQA Highett
NDISL Amberley

Other

New Zealand Defence Liaison Officer (Doc Data sheet only)

SWITZERLAND

Dr. H. Boesch - Swiss Aircraft Factory, Emmen

UNITED STATES OF AMERICA

P.H. Hutton - Battelle Pacific Northwest Laboratories

SPARES (10 copies)
TOTAL (67 copies)

AD-A196 364

AL 149
REVISED DECEMBER 87

DEPARTMENT OF DEFENCE

DOCUMENT CONTROL DATA

PAGE CLASSIFICATION
UNCLASSIFIED
PRIVACY MARKING

1a. AR NUMBER	1b. ESTABLISHMENT NUMBER	2. DOCUMENT DATE	3. TASK NUMBER
AR-004-585	ARL-MAT-R-120	JANUARY 1988	AIR 85/038

4. TITLE	5. SECURITY CLASSIFICATION	6. No. PAGES
THE DEVELOPMENT OF ACOUSTIC EMISSION FOR STRUCTURAL INTEGRITY MONITORING OF AIRCRAFT	(PLACE APPROPRIATE CLASSIFICATION IN BOX(S) IE. SECRET (S), CONFIDENTIAL (C), RESTRICTED (R), UNCLASSIFIED (U).) U DOCUMENT, U TITLE, U ABSTRACT	40
		7. No. REFS. 43

8. AUTHOR(S)	9. DOWNGRADING/DELIMITING INSTRUCTIONS
C.M. SCALA, S.J. BOWLES, I.G. SCOTT	NOT APPLICABLE

10. CORPORATE AUTHOR AND ADDRESS	11. OFFICE/POSITION RESPONSIBLE FOR
AERONAUTICAL RESEARCH LABORATORY P.O. BOX 4331, MELBOURNE VIC. 3001	SPONSOR RAAF SECURITY - DOWNGRADING - APPROVAL -

12. SECONDARY DISTRIBUTION (OF THIS DOCUMENT) Approved for Public Release

OVERSEAS ENQUIRIES OUTSIDE STATED LIMITATIONS SHOULD BE REFERRED THROUGH ASDIS, DEFENCE INFORMATION SERVICES BRANCH, DEPARTMENT OF DEFENCE, CAMPBELL PARK, CANBERRA, ACT 2601

13a. THIS DOCUMENT MAY BE ANNOUNCED IN CATALOGUES AND AWARENESS SERVICES AVAILABLE TO.....
No limitations

13b. CITATION FOR OTHER PURPOSES (IE. CASUAL ANNOUNCEMENT) MAY BE [X] UNRESTRICTED OR [ ] AS FOR 13a.

14. DESCRIPTORS		15. DRDA SUBJECT CATEGORIES
Acoustic emissions	Macchi aircraft	0094J
Fatigue crack growth;	Mirage aircraft	
Nondestructive testing;		
Signal processing; Australia, (edc)		

16. ABSTRACT This paper reviews procedures for distinguishing between acoustic emission (AE) from fatigue crack propagation and from spurious sources in aircraft applications. Particular emphasis is placed on the development at the Aeronautical Research Laboratory (ARL) of procedures applicable during AE monitoring of complex-shaped components. Firstly, procedures to eliminate extraneous sources are evaluated, including the use of guard sensors and source location systems. The capabilities of additional signal-processing (which in principle can range from adaptive to non-adaptive) for identifying and locating AE from fatigue crack propagation are then evaluated. The problems in applying adaptive processing are illustrated by AE results from a Macchi aircraft in-flight and a Mirage aircraft during full-scale fatigue testing. The

PAGE CLASSIFICATION
UNCLASSIFIED

PRIVACY MARKING

THIS PAGE IS TO BE USED TO RECORD INFORMATION WHICH IS REQUIRED BY THE ESTABLISHMENT FOR ITS OWN USE BUT WHICH WILL NOT BE ADDED TO THE DISTIS DATA UNLESS SPECIFICALLY REQUESTED.

16. ABSTRACT (CONT.)

ARL development of semi-adaptive processing based on background research on AE sources, sensors, calibration and other techniques is also described. The successful application of this processing to the Mirage test above is then detailed, and the value of using reduced adaptation in processing is demonstrated. Finally, factors affecting future in-flight AE monitoring are discussed.

17. IMPRINT

AERONAUTICAL RESEARCH LABORATORY, MELBOURNE

18. DOCUMENT SERIES AND NUMBER	19. COST CODE	20. TYPE OF REPORT AND PERIOD COVERED
AIRCRAFT MATERIALS REPORT 120	31 1256	

21. COMPUTER PROGRAMS USED

22. ESTABLISHMENT FILE REF. (S)

M1/8/615

23. ADDITIONAL INFORMATION (AS REQUIRED)

END

DATE

FILMED

8 8-